Sequential dark fermentation and microbial electrolysis cells for hydrogen production: Volatile fatty acids influence and energy considerations

Jose Antonio Magdalena, María Fernanda Pérez-Bernal, Nicolas Bernet, Eric Trably

SEQUENTIAL DARK FERMENTATION AND MICROBIAL ELECTROLYSIS CELLS FOR HYDROGEN PRODUCTION: VOLATILE FATTY ACIDS INFLUENCE AND ENERGY CONSIDERATIONS

Jose Antonio Magdalena[1,2,*], María Fernanda Pérez-Bernal[1], Nicolas Bernet[1], Eric Trably[1]

[1] INRAE, Université de Montpellier, LBE, 102 avenue des Étangs, 11100 Narbonne, France

[2] Vicerrectorado de Investigación y Transferencia de la Universidad Complutense de Madrid, 28040 Madrid, Spain

*Corresponding author: jose.antonio-magdalena.cadelo@inrae.fr

ABSTRACT

Hydrogen production from food waste by coupling mesophilic dark fermentation (DF) and microbial electrolysis cells (MEC) was investigated. The main objectives were i) study the metabolic patterns in DF, ii) fill the gap of knowledge regarding the effect of different DF metabolic profiles in MECs and iii) calculate the energy output of the coupling. pH and temperature screening showed the highest hydrogen production at acidic pH 5.5-6 (72 ± 20 mL H_2/g CODin) and butyrate-enriched profile (C2/C4, 0.5-0.6) contrasting with an acetate-enriched profile (C2/C4, 1.8-1.9) and 36 ± 5 mL H_2/g CODin at pH 7. Assessment of the pH 7 effluents in MECs resulted in a higher hydrogen yield (566-733 mL H_2/g CODin) and VFAs removal (84 - 95%) compared to pH 5.5 effluents (173-186 mL H_2/g CODin and 29-59 %, respectively). The energy output showed similar absolute values for the batches at pH 7 and 5.5 (25-30 KJ).

KEYWORDS: Bioeconomy; dark fermentation; energy; biohydrogen; microbial electrolysis cells; volatile fatty acids

1. INTRODUCTION

In recent times, research efforts have aimed at tapping into hydrogen enormous potential to tackle the industry decarbonisation. This enormous challenge requires the combined use of different renewable technologies, which should unavoidably co-exist to gradually achieve the so-called *climate neutrality*. In this context, clean hydrogen has been clearly identified as a priority area due to its potential to bridge the gap as biofuel for transport alongside renewable energy storage. In fact, the European Commission predicts a momentous growth of the hydrogen share in Europe from the current (< 2%) to 13-14% by 2050 (European Commission, 2020). The importance of hydrogen in this strategic change of paradigm lies in its low carbon footprint, its high energy content (120 MJ/Kg), and the fact that it is considered as the cleanest energy carrier, only producing water as by-product (Tian et al., 2019).

The incipient growth of the hydrogen sector may go hand-in-hand with the development of biological hydrogen production. These sustainable and inexhaustible bioprocesses might solve the dual problem of waste disposal and energy generation since organic residues can be employed as substrate. Amongst these bioprocesses, dark fermentation (DF) appears to be the most promising. DF does not require light energy and presents lower energy demands than conventional carbon based processes. However, the relatively low hydrogen yield is the main bottleneck encountered, which still prevents the scaling up of this technology (Tapia-Venegas et al., 2015). In fact, only 30-35% of the energy in DF processes can be converted to hydrogen (Khongkliang et al., 2017), because of the thermodynamic limit of 4 moles hydrogen per mole of glucose (Koul et al., 2022). Additionally, a large fraction of the organic matter is hydrolysed and transformed into volatile fatty acids (VFAs), which are the main co-products present in the liquid effluent (Zhen et al., 2017). An interesting solution to improve this drawback is to couple the DF process with microbial electrolysis cells (MECs), in which a very small energy input (-300 mV vs SHE) is required to break the thermodynamic barriers for the conversion of “dead-

end" metabolites (*i.e.* acetate) into hydrogen (Zhen et al., 2017). This two-step configuration would enhance the substrate degradability and the overall hydrogen yield, with a possible theoretical output of 12 moles hydrogen/mole glucose. A previous research considering this coupling showed a high variability of MEC performances depending on the substrates assessed (Marone et al., 2017). As a matter of fact, carbon degradability and substrate conversion to hydrogen relied on the VFAs spectrum fed into the MEC process. Thus, one limitation of using MECs after DF is the diverse and unstable VFA profile that might be obtained during the DF step. Operational parameters, including organic loading rate, retention time, temperature or pH affect the VFAs distribution. In fact, both pH and temperature values (Zagklis et al., 2021) play an important role in DF affecting the optimum activity of microbes and enzymes (*i.e.* hydrogenase enzyme) and finally, metabolic pathways.

This experimental study was designed for studying the metabolic patterns at different pH values and temperatures in DF and fill the gap of knowledge regarding the effect of different VFAs profiles as feedstock in MEC reactors, using food waste (FW) as substrate. Additionally, the energy output of the coupling was calculated to identify the strengths and weaknesses of the coupling.

2. MATERIAL AND METHODS

2.1. Seed inoculum and substrate

The aerobic inoculum employed in this experimental study was collected from the activated sludge system at the wastewater treatment plant of Narbonne (France). The sludge was subjected to a freeze-drying process and stored at -80 °C to avoid changes in dynamic populations and for a better reproducibility of the results (Dauptain et al., 2021). Characterization of the sludge revealed a VS/TS ratio of 0.97.

Since FW has higher carbohydrate content and biodegradability than other organic wastes, high hydrogen production potential and rate are generally achievable. FW was stored frozen at -20 °C to avoid changes in its composition over time as described in previous research (Noguer et al., 2022). Waste components were cut in small pieces and mashed with a kitchen blender. Once homogenised and prior fermentation in the digester, the FW was thermally pretreated at 70 °C for 1 h. This step was carried out to anticipate further use at industrial scale, as required by the European Union (EU) Regulation 142/2011 (The European Comission, 2011). Afterwards, the feedstock was sieved through 2 mm mesh. Finally, characterization revealed a VS/TS ratio of 0.96 and a total and soluble Chemical Oxygen Demand (tCOD and sCOD) relation of sCOD/tCOD = 0.21.

2.2. DF experiments: pH and temperature screening

For pH screening, Biohydrogen potential batch experiments (BHPs) were carried out in 0.5 L reactors with 0.2 L working volume (Carrillo-Reyes et al., 2020). The ratio $VS_{substrate}/VS_{inoculum}$ was 8.7. Initial pH was adjusted at different pH values *i.e.* 5, 6, 7, and 8 by using 2 M NaOH or 12.18 M HCl. To maintain pH within the range desired, 0.16 M MES buffer was used for pH 5 and 6, and 0.16 M $NaHCO_3$ at pH 7 and 8. Prior to fermentation, aerobic sludge was pretreated at 90 °C for 15 min to prevent any methanogenic activity (Parthiba Karthikeyan et al., 2018). After inoculation all flasks were flushed with nitrogen for 15 min to reach strictly anaerobic conditions and subsequently capped with a rubber stopper and incubated at 37 °C. Batch tests were performed in triplicate. Gas production was monitored every 2 h with an automatic microgas chromatograph (MicroGC, SRA l-GC R3000) equipped with two columns: a Molesieve 5A 10 m column running at 80 °C, 30 PSI with argon as carrier gas (channel A) and a PoraPlot U (PPU) 8 m column running at 70 °C, 20 PSI with helium as carrier gas (channel B), for H_2, O_2, N_2, CH_4 and CO_2 analyses, respectively. Both channels were equipped with a

micro-thermal conductivity detector (TCD) set at 90 °C. Gas production was estimated by pressure measurement.

For the temperature screening, 3 L reactors (Applikon Bio 3 L, Getinge, Göteborg, Sweden) with 2 L working volume were employed. Temperature and pH were controlled and monitored at 25, 37 and 50 °C and pH 5.5 and 7, respectively, by means of an automatic system (M300, Mettler Toledo, Greifensee, Switzerland). Temperature was measured with an immersed probe and regulated by means of a heating blanket, while pH was measured by an in situ probe and regulated with 3 M NaOH. Mixing was ensured by mechanical stirring (350 rpm). Pressure was regulated with a control device combining a pressure sensor (LEO3, Keller, Winterthour, Switzerland) and a peristaltic pump (Masterflex L/S 7554-85, Cole Parmer, Vernon Hills, IL, USA) following a two-band control law between 1030 and 1070 mbar. Gas production was measured through the pressure variations inside the fermenter and by using the operating time of the calibrated peristaltic pump. Produced gas volumes were normalized (T = 0 °C and p = 1 atm).

At the end of both screenings, effluents were sampled for pH and VFAs analysis and centrifuged at 8,000 rpm for 15 min. The liquid phase was stored at -20 °C for its use in the MECs (as described in Section 2.3).

2.3. Microbial electrolysis cells (MECs)

The reactor employed for hydrogen production via MEC from fermentation effluents was a cylindrical two-chamber reactor. Each chamber had a working volume of 0.85 L. The anode consisted of a carbon felt (G600A, AvCarb Material Solutions, U. S.) pretreated (Paul et al., 2018) with a projected surface of 70 cm^2, screwed onto a 2 mm diameter titanium road (TI007910/13, Goodfellow SARL, France) as electron collector. The cathode was made of 90 % Platinum-10 % Iridium mesh (Heraeus PSP S.A.S., France). Each chamber was sealed with silicone grease and a ring of stainless steel to ensure tightness. The membrane selected to

separate both chambers was a cation exchange membrane (CEM, Fumasep FKB-PK, FuMA-Tech BWT GmbH, Germany) with a thickness of 130 µm. The experiments were conducted using a Silver/Silver Chloride (Ag/AgCl) Reference Electrode saturated with KCl (+199 mV vs. SHE) (Origalys Electrochem SAS, France). Experimental tests were conducted at a set temperature of 37 °C and 250 rpm. MEC tests were carried out in series and in duplicate using the same reactor.

Firstly, two chronoamperometric cycles (CA) of 7 days each were performed to enrich the anode with an electroactive biofilm. The enrichment cycles were performed using a synthetic medium. The following composition was used at the anode: 1 g/L acetic acid, 2 g/L NH_4Cl, 0.5 g/L K_2HPO_4, 9.76 g/L MES (2-[N-morpholino] ethane sulfonic acid) buffer, and 10 mM 2-brome-ethane sulfonate (BES) to prevent methane production. The medium at the cathode had the same composition than in the anodic compartment, but neither acetate nor BES were added. Afterwards, the anodic chamber was inoculated with aerobic sludge (10% v/v), and the anode potential was fixed at +245 mV vs. Ag/AgCl using a Potentiostat VMP3 (BioLogic Science Instruments, France) controlled by the software EC-Laboratory v.10.1. For all experiments, the current density was recorded every 10 min. Cyclic voltammetry (CV) was performed at a scan rate of 1 mV/s within the potential range of -0.7 V - +0.3 V mV vs Ag/AgCl at the beginning and the end of each enrichment cycle (control-CV) to monitor the biofilm development.

After the enrichment period, the medium in the anode was almost completely replaced (~ 90 % v/v) by real effluents. First, two batches with fermentation effluent obtained at pH 7, and then two batches with effluent obtained at pH 5.5. The pH was adjusted to 7.0 in both cases for the MEC process, and the system was flushed with nitrogen gas to establish anaerobic conditions. The volume of hydrogen production was measured using a Ritter counter connected to the cathodic chamber, the gas produced was stored in a Tedlar® sample gas bag. The current density, gas composition, and volatile fatty acids (VFAs) concentration were monitored along

the experimental time. Duration of experiments lasted for at least three chronoamperometric cycles (21 days), and were stopped either when VFAs were depleted or increasing methane concentrations were detected.

2.4. Analytical measurements

Total solids (TS) and volatile solids (VS) were calculated according to standard methods (Eaton et al., 2005). Total and soluble chemical oxygen demand (tCOD and sCOD respectively) were measured by using commercial kits (Lovibond, Germany). Prior to metabolite analysis, samples were centrifuged 15 min at 13,000 g and filtered through 0.2 μm (nylon filter 15121499, Fisher Scientific, Waltham, MA, USA). VFAs were determined by using a gas chromatograph (GC-580 Clarus, Perkin Elmer, Waltham, MA, USA) equipped with an automatic sampler, an Elite-FFAP column and a flame ionization detector (FID) at 280 °C. The carrier gas was N_2 circulating at a flow rate of 6 mL/min. Other metabolites from the fermentative broth such as ethanol, lactate, succinate or residual sugars were measured by HPLC (High Performance Liquid Chromatography). The device was composed of a protective precolumn (Microguard cation H refill catbridges, Biorad, Hercules, CA, USA) and an HPX-87H column (300 × 7.8 mm, Biorad, Hercules, CA, USA) running at 35 °C coupled to a refractive index detector (R410, Waters, Milford, MA, USA) at 45 °C. 4 mM H_2SO_4 was used as mobile phase at a rate of 0.3 mL/min.

2.5. Calculations

Substrate degradation into metabolites (% COD-met/CODin) was assessed by calculating the ratio of the sum of the COD of each metabolite produced to the COD of the substrate introduced into the reactor, as follows (Equation (1)):

$$\% \frac{\text{CODmet}}{\text{CODin}} = \frac{COD_{C2}+COD_{C3}+COD_{i-C4}+COD_{C4}+COD_{i-C5}+COD_{C5}+COD_{i-C6}+COD_{C6}+COD_{Lact}+COD_{EtOH}}{COD_{in}} \quad \text{Eq (1)}$$

with COD_{Cn}, COD_{Lac}, and COD_{EtOH} corresponding to the stoichiometric COD of each compound required to completely breakdown each of these acids to carbon dioxide. VFAs

removal was calculated according to Eq. 2, where CODin is the total organic matter fed into the system and CODout is the total organic matter recovered in the effluent:

$$\text{VFAs removal (\%)} = \frac{VFAs_{in} - VFAs_{out}}{VFAs_{in}} \cdot 100 \quad \text{Eq (2)}$$

The organic acids produced during fermentation were converted to acetic acid equivalents using Eq. 3 (Murali et al., 2021):

$$VFAs_{aa-eq} = C2 + \left(C3 \cdot \frac{TO_{C3}}{TO_{C2}} \cdot \frac{MW_{C2}}{MW_{C3}}\right) + \left(C4 \cdot \frac{TO_{C4}}{TO_{C2}} \cdot \frac{MW_{C2}}{MW_{C4}}\right) + \left(C5 \cdot \frac{TO_{C5}}{TO_{C2}} \cdot \frac{MW_{C2}}{MW_{C5}}\right) \quad \text{Eq (3)}$$

where MW refers to the molecular weight of acetate (MW_{C2}), propionate (MW_{C3}), butyrate/isobutyrate (MW_{C4}) and valerate/isovalerate (MW_{C5}) and TO_{CX} refers to the theoretical amount of oxygen required to completely breakdown each of these acids to carbon dioxide.

The performance of the MEC reactors was compared based on: Coulombic efficiency (CE), cathodic hydrogen recovery (r_{cat}), hydrogen production rate (L H_2/Ld), maximum current density (A/m^2) and global yield (r_{H2}). CE was calculated as n_{ce}/n_{th}, where n_{ce} was the number of hydrogen moles that could be recovered based on the measured current and n_{th} was the theoretical maximal production based on VFAs removal. R_{cat} was calculated as n_{H2}/n_{ce}, where n_{H2} is number of moles of hydrogen produced at the cathode. Finally, r_{H2} was calculated by multiplying r_{cat} and CE.

Energy considerations are crucial to assess the feasibility of the coupling of these two bioprocesses. Based on our experimental results, the energy output (E0, KJ) generated in the fermentation (first step) was calculated according to Equation (4) (Jia et al., 2020):

$$E_1 = \rho H_2 \cdot qH_2 \cdot V_1 \quad \text{Eq (4)}$$

where E1 is the generated energy of hydrogen from DF (KJ); ρH_2 is the hydrogen density hydrogen (0.0899 kg/m^3); qH_2 is the calorific value of hydrogen ($1.43 \cdot 10^5$ KJ/Kg); and V_1 is the hydrogen yield from DF (m^3).

Hydrogen energy from the MEC was calculated as follows:

$$E_2 = \rho H_2 \cdot qH_2 \cdot V_2 \quad \text{Eq (5)}$$

where E_2 is the generated energy of hydrogen from MEC (kJ), and V_2 is the hydrogen yield from MEC (m^3).

2.6. Statistical analysis

The results are given as the average ± standard deviation for descriptive statistics. Analysis of variance (ANOVA) was carried out for comparisons of DF and MEC data obtained in all the experiments. The level of significance was set at $p < 0.05$.

3. RESULTS AND DISCUSSION

3.1. Dark Fermentation

3.1.1. Selection of the most suitable storage method for the inoculum

BHPs were carried out using both fresh and freeze dried aerobic sludge as inoculum to evaluate hydrogen production. The aim of these batch assays was to validate the freeze drying method reported by Dauptain et al. (2021) as an appropriate storage method for the aerobic sludge inoculum. Additionally, the influence of a heat shock pretreatment to the sludge at 90 °C for 30 min prior fermentation was assessed. Since aerobic sludge contains less strict anaerobic methanogenic archaea than anaerobic sludge, its use can be beneficial to promote hydrogen production. Similar yields were obtained with both kind of inoculum. Hence, prior to DF at the different pH values, the seed inoculum was freeze-dried and subjected to a heat shock pretreatment at 90 °C for 30 min, to homogenize the starting conditions of each assay

3.1.2. Effect of initial pH value on biohydrogen production and VFAs profile

To evaluate the hydrogen potential and metabolic patterns using FW as substrate, BHPs tests were carried out at pH values ranging from 5 to 8. At these conditions, as shown in Fig. 1A, the hydrogen production was clearly influenced by the initial pH. Hydrogen produced was maximum at pH 6 (136.0 ± 5.3 mL H_2/g VS_{in}), followed by pH 5 (64.2 ± 0.2 mL H_2/g VS_{in}), pH 7 (55.0 ± 3.6 mL H_2/g VSin), and pH 8 (38.3 ± 10.2 mL H_2/g VS_{in}) (Figure 1 A, p-value < 0.05). Final pH values at the end of the fermentation were 4.4 ± 0.1, 5.4 ± 0.1, 6.9 ± 0.1, and 7.2 ± 0.1, for assays carried out at pH 5, 6, 7 and 8, respectively. FW residues are often rich in soluble carbohydrates leading to high hydrogen yields when appropriate process parameters (pH and temperature) are employed. The high hydrogen yield observed at pH 6 compared to 5 and neutral and slightly basic pH values (pH 7 and 8) might have been linked to the original pH from the inoculum, which was close to 6. Consistently, a similar study using FW as substrate reported the highest maximum H_2 yield (1.63 mol H_2/mol $hexose_{added}$) at low pH (5.3), whereas the lowest yield was 0.88 mol H_2/mol $hexose_{added}$ at pH 7 (Lee et al., 2014). Following the same trend, a recent investigation showed the effect of initial pH from 4 to 11, concluding that the initial pH of 5 (followed by pH 6) produced the highest cumulative hydrogen yield (70 and 60 mL H_2/g VSS, respectively) (Tang et al., 2022).

Total organic acids produced (g COD/L) were minimum and significantly lower (p-value < 0.5) at pH 5 (4.5 ± 0.2) than at pH 6, 7 and 8 (6.0 ± 0.1, 6.3± 0.6 and 6.1± 0.2, respectively) (Figure 1B). Consequently, organic matter conversion into metabolites from the organic matter fed in the system was maximum at these pH values (59.6 ± 0.9, 61.0 ± 1.9 and 62.9 ± 0.1, respectively). With regard to the organic acid profile obtained, no sugars nor lactate were detected, suggesting that they were consumed during DF. Organic acids distribution was dependent on the pH assessed. Acetate increased significantly (p-value < 0.5) from 24.5 ± 3.5 % at pH 5 and 36.4 ± 1.4 at pH 6 to 51.9 ± 7.5 and 53.4 ± 4.0 % at pH 7 and 8, respectively,

being the most abundant product in the latter experiments. Conversely, butyrate concentration was maximized at pH 5 and 6 (57.3 ± 1.1 and 44.3 ± 1.0) with respect to the concentrations obtained at pH 7 and 8 (27.4 ± 0.5 and 30.6 ± 2.2). This metabolite profile dependence on pH values agreed with what it is commonly found in literature where butyrate concentration tended to increase whilst acetate concentration decreased at acidic pH values (Lee et al., 2014). Acetate and butyrate represented around 80% of the COD transformed in all the effluents regardless the pH value assessed. Propionate was only present at pH 7 and 8 in concentrations ranging from 6 to 20 % in COD basis and other compounds such as iso-butyrate, iso-valerate or ethanol were only present in a minor extent.

Hence, the use of different process pH (acidic or neutral/basic) resulted in effluents with a different composition in terms of VFAs distribution. From this point, one effluent from each pH value was studied: i) a process pH value in the acidic range (5.5) to favour butyrate production and ii) a process pH value in the neutral range (7) to favour acetate production.

3.1.3. Effect of temperature value on biohydrogen production and VFAs profile

Finding a trade-off between organic acids and hydrogen production in DF is crucial to select the optimum operational conditions for hydrogen production and at the same time to obtain an effluent with an appropriate organic acid distribution to feed a MEC.

The highest hydrogen production was achieved at 37 °C for both pH values (73 ± 21.2 mL H_2/g VSin at pH 5.5 and 53.5 ± 10.6 mL H_2/g VSin at pH 7). Both temperatures of 25 and 50 °C did not improve the hydrogen yield of the process, resulting in values as high as 20 mL H_2/g VSin (in the case of 25 °C). The fact that the inoculum was collected from a mesophilic source might have been decisive, explaining the low hydrogen yields observed at both 25 and 50 °C. Interestingly, organic matter conversion into organic acids achieved its highest value at 25 °C with a pH of 5.5 (51.6 ± 1.2 % COD-met/CODin) and 7 (66.1 ± 2.4 % COD-met/CODin).

However, these results were very similar to those found at 37 °C (49.0 ± 0.5 % and 65.1 ± 2.9 % for pH 5.5 and 7, respectively) (Figure 2). At thermophilic conditions (50°C) the lowest hydrogen and organic acids yields were observed regardless of the pH value. With regard to the organic acid profile, it was more influenced by the process pH than the temperature. In fact, at pH 5.5 and all temperatures assessed, butyrate production was as important as acetate. In contrast, at pH 7, acetate dominated the organic acids profiles followed by butyrate and propionate. Interestingly, as observed at pH 5.5, the profile obtained at pH 7 was similar regardless of the temperature evaluated. This fact highlighted that the process pH was more determining than temperature to shape the organic acid distribution.

Overall, the highest hydrogen yields were achieved at 37 °C, being maximized at pH 5.5. Meanwhile, organic matter conversion into organic acids was optimum at 25 and 37 °C and pH 7. This result indicated that using 25 °C along with the use of neutral pH could be an interesting approach to promote organic acid productions whilst increasing the cost-effectiveness of the DF process due to the low process temperature employed. As the results were nevertheless quite similar, the effluents obtained at 37 °C were further used in MEC to employ the same temperature conditions in both bioprocesses.

3.2. Microbial electrolysis cells

3.2.1 Current density generation and Coulombic efficiency

After two chronoamperometric cycles with synthetic medium, an electroactive biofilm was successfully developed as evidenced by the cyclic voltammetry (CV) analysis made at the beginning and end of the enrichment process. The maximal current densities achieved were around 5 A/m^2, which are the values expected when using acetate as substrate (3-5 A/m^2) as reported by Marone et al. (2017). For assays with real effluents (or DF effluents), the highest current densities (J, A/m^2), recorded during CAs, were achieved with the fermentation effluents obtained at pH 7, and reached a maximum at the beginning of the experiment (1.36 ± 0.39 and

1.19 ± 0.49 A/m^2, for batch A and B, respectively) when both, acetate and propionate were available. The high initial current densities recorded at the beginning of the batch with real effluent from DF at pH 7, were similar to current densities obtained during enrichments. This fact was consistent since both, real and synthetic effluents, were rich in acetate. However, for DF effluents produced at pH 5.5, the initial high current density peaks were not registered and the values remained in the range of those found for pH 7 when acetate was depleted (0.69 ± 0.27 and 0.52 ± 0.28 A/m^2). As effluents obtained at both pH showed similar acetate concentrations but different butyrate contents with a considerably higher value at pH 5.5, a possible inhibiting phenomenon might have occurred (See Section 3.2.2). With regard to the Coulombic Efficiency (CE), results obtained from the tested effluents were remarkably higher for acetate-rich effluents coming from DF at pH 7 over those coming from DF at pH 5.5 (83-91 % vs 8-12%). In this sense, the CE diminution was entirely attributed to the shift in the organic acid profile even though there is other phenomena observed in long time operating MECs such as efficiency losses due to some undesired electron sinks reactions of alternative metabolisms (Koul et al., 2022). In this sense, organic acids might have been consumed by electrochemically inactive fermentative bacteria that gradually increased on the MEC colonizing the bioanode. Still, the CEs observed throughout the experimental time when acetate was promoted (DF from pH 7) were higher than those obtained in other studies using fermented effluents as substrate to feed MECs. For instance, a study evaluating six different fermented residues for hydrogen production in MECs resulted in an average CE of 62.7 ± 10.4 % (Marone et al., 2017). Overall, the CE and J evidenced the influence of the organic acid profile in MEC performance

3.2.2 Organic acids removal

The organic acids removal efficiency observed in MECs ranged from 84-95 % in the effluents from pH 7 and from 29-59 % in the effluents from pH 5.5. This variability was attributed to the

initial organic acid distribution and the experimental time. Effluents from DF carried out at pH 7 (Figure 3, A-B) had acetate as most abundant metabolite followed by butyrate and propionate. Additionally, all effluents presented other acids such as the isoforms of butyrate and valerate (accounting for less than 10 % of the COD), which remained unconsumed regardless of the effluent assessed. For the first experiment assessed (Figure 3-A), acetate was preferentially consumed during the first days of experiment (up to day 10), and only when it was depleted, propionate and butyrate consumption took place. This result coincided with the findings of Yang et al., (2015), who evaluated these acids independently using synthetic media and evidenced the preference for acetate to be consumed. However, for the second effluent evaluated (Figure 3-B), acetate, propionate and butyrate consumption occurred simultaneously (up to day 20), and it was even accelerated when acetate was depleted. The consumption of these three acids at the same time might be linked to the fact that the experiments were carried out in series. Hence, an adaptation likely occurred and the system was able to degrade not only acetate, but also propionate and butyrate at the given concentrations. Overall, these results showed that acetate could be easily oxidized by anode bacteria in MEC, while butyrate and propionate are harder to be oxidized to the same degree.

Regarding the effluents from DF carried out at pH 5.5, the COD obtained as metabolites consisted mainly of butyrate followed by acetate. The experiment pH 5.5-A (Figure 3-C) was running for 21 days and was stopped due to increasing methane concentrations registered in the gas phase. It must be highlighted that the butyrate concentration employed was notably higher than that evaluated in other studies. For instance, Flayac et al., (2018) assessed the interaction of bacterial species for the conversion of butyric acid into electrical current. For this purpose, the authors employed butyrate concentrations around 0.3-0.4 g/L (0.5-0.7 g COD/L) achieving an average butyrate removal of 47.3 ± 21.9 in 30 days. In the present study, the batches from pH 7 (Figure 3, A-B) behaved similarly (removals of 50 and 100 %) in a similar period of time.

With respect to pH 5.5, in the first batch (Figure 3-C) butyrate was barely consumed (removal of 10 %) since acetate was still available in the medium. However, the second replicate (Figure 3-D) achieved a butyrate removal of 42 % in 46 days using a higher butyrate concentration (2-3 fold) than one employed by Flayac and co-workers. It is important to highlight at this point that the bioanode was developed using acetate, thus favouring acetate consumers, and for this reason, an enrichment with butyrate might be expected to enhance the butyrate removal rates.

3.2.3 Hydrogen generation and yield in the MEC

Performance indicators of the hydrogen production in the MEC process are shown in Table 1. The highest hydrogen yield was achieved with the effluents coming from DF at pH 7 (733.14 – 566.28 mL H_2/ g CODin) compared to the ones coming from DF carried out at pH 5.5 (172.98 – 186.07 mL H_2/ g CODin) ($p < 0.05$). Hydrogen yields found in literature are quite diverse as they often result from the high influence of variables such as the nature of the feedstock employed in fermentation, the acid organic profile obtained after fermentation, the operational conditions imposed in the MEC, the electroactive microbial communities and the electrodes material. In literature, hydrogen yields ranged from 219 mL H_2/g COD up to 1500 mL H_2/g COD (Chookaew et al., 2014; Khongkliang et al., 2019; Lalaurette et al., 2009; Marone et al., 2017). Hence, it can be inferred the high influence that the organic acid profile fed to the MECs exerts on the final hydrogen yield. The highest proportion of short-chain organic acids (acetate and propionate) in the effluent from DF at pH 7 led to a better MEC performance (r_{H2} 52-54%) when compared to the effluent from DF at pH 5.5 (r_{H2} 3-7%) which had a higher relative abundance of butyrate. Likewise, the higher presence of butyrate in pH 5.5 batches explained the lower yield per g VFAaa-eq, as the major extent of this compound remained unconsumed.

Finally, it should be highlighted that there was increasing methane production detected at longer experimental times in all MEC tests (<10%, data not shown). Production of methane lowers hydrogen production either through conversion of acetate to methane or through

hydrogenotrophic methanogenesis. This is a persisting problem in MECs application for hydrogen production that might be solved by choosing an appropriate strategy, namely chemicals additions, the use of pure cultures or employing stress operational conditions (i.e. low pH and temperature operation, periodic aeration and exposure of reactor or electrodes to air) (Kadier et al., 2018).

3.4 Energy considerations

In the present work, hydrogen production yields in MECs varied according to the pH conditions in DF. On one hand, pH 7 promoted a suitable acetate-rich effluent for hydrogen production in MECs but resulted in a very low hydrogen yield during the first DF step. On the other hand, the use of pH 5.5 produced higher hydrogen yields in DF but scarce exploitation of butyrate in the MEC process, which was the main metabolite in the DF effluent. For this reason, the energy output of the coupled process is crucial to decide which conditions should be applied to optimize the global process and which aspects should be enhanced. Figure 4 shows a scheme of the energy balances applied to the DF and the MEC process for the different batches.

The Energy output (E_0) was clearly influenced by the process pH in DF, whose value increased 2-fold at pH 5.5 (E_0=18.5 KJ) compared to pH 7 (E_0=7.4 KJ). This result was expected according to the yields obtained in Section 3.1.3. Following with the effluents from pH 5.5, Batches C and D showed low energy generation in MECs (E_0 7.1 and 9.6 KJ, respectively), which evidences the limitations of the MEC process when butyrate is fed into the system. Conversely, the acetate-rich effluent generated from DF at pH 7 resulted in a higher energy production in the MEC stage (E_0 23.5 and 11.2 KJ, respectively), especially in Batch A, due to the higher acetate availability in this effluent. It is important to highlight at this point, that even though results might seem similar in terms of total energy produced, the amount of energy per g CODin in the MEC was 4-fold higher when employing the effluents from pH 7 (7.31-9.45 KJ/g CODin) compared to the ones coming from pH 5.5 (2.22-2.39 KJ/ g CODin). The results

obtained from pH 5.5, in which DF for hydrogen production was optimized, were consistent with the ones obtained by Jia et al. (2020), who generated more energy during the DF process (8.34 KJ) than in the MEC (1.48 KJ) when establishing the DF at pH 6. However, it can be inferred from this result that process parameters (such as pH) can direct the energy production to either of the processes involved in the coupling.

Overall, batches A (pH 7), C and D (pH 5.5) showed similar total energy productions (25-30 KJ) when considering the coupling DF + MEC. With regard to pH 5.5, effluent exploitation in the MECs field should be investigated to enhance the overall process yields. Future strategies should be directed to enhance butyrate degradation, which appears as a key step to enhance the energy output at pH 5.5.

4. CONCLUSIONS

Process pH shaped DF effluent impacting on MEC performance. In this regard, acetate, more abundant at pH 7, was preferentially consumed in the MEC, whereas the lack of this compound and a high availability of butyrate at pH 5.5 resulted in lower hydrogen yields in the MEC. The net energy productions considering the coupling suggested similar performances in the present study for both pH values assessed, although normalizing the units (KJ/gCODin) clearly showed a high efficiency of the MEC step when acetate led the VFAs profile. Butyrate consumption in MECs appears as a key step to enhance overall process efficiency.

E-supplementary data of this word can be found in online version of the paper.

Acknowledgments: This study was carried out in the framework of the HyDS Project (part of the ERDF-REACT-EU- H2VERT project). Jose Antonio Magdalena would like to thank the Complutense University of Madrid for the financing of his contract at LBE-INRAE (France), with funds of the Ministry of Universities for the requalification of the Spanish University System for 2021–2023 (Modality 1. Margarita Salas), coming from the European Union-Next generation EU funding.

Author Contributions: Conceptualization, J.A.M. and E.T.; validation, F.P.B, N.B. and E.T.; investigation, J.A.M. and F.P.B.; writing—original draft preparation, J.A.M.; writing—review and editing, J.A.M., F.P.B.; supervision, N.B. and E.T.; project administration, N.B. and E.T.; funding acquisition, E.T. All authors have read and agreed to the published version of the manuscript.

REFERENCES

Carrillo-Reyes, J., Buitrón, G., Moreno-Andrade, I., Tapia-Rodríguez, A.C., Palomo-Briones, R., Razo-Flores, E., Aguilar-Juárez, O., Arreola-Vargas, J., Bernet, N., Braga, A.F.M., Braga, L., Castelló, E., Chatellard, L., Etchebehere, C., Fuentes, L., León-Becerril, E., Méndez-Acosta, H.O., Ruiz-Filippi, G., Tapia-Venegas, E., Trably, E., Wenzel, J., Zaiat, M., 2020. Standardized protocol for determination of biohydrogen potential. MethodsX 7, 100754. https://doi.org/https://doi.org/10.1016/j.mex.2019.11.027

Chookaew, T., Prasertsan, P., Ren, Z.J., 2014. Two-stage conversion of crude glycerol to energy using dark fermentation linked with microbial fuel cell or microbial electrolysis cell. N. Biotechnol. 31, 179–184. https://doi.org/10.1016/j.nbt.2013.12.004

Dauptain, K., Schneider, A., Noguer, M., Fontanille, P., Escudie, R., Carrere, H., Trably, E., 2021. Impact of microbial inoculum storage on dark fermentative H_2 production. Bioresour. Technol. 319, 124234. https://doi.org/10.1016/j.biortech.2020.124234

Eaton, A.D., Clesceri, L.S., Greenberg, A.E., Franson, M.A.H., 2005. Standard methods for the examination of water and wastewater. Am. public Heal. Assoc. 21, 1600.

European Commission, 2020. Communication COM/2020/301: A hydrogen strategy for a climate-neutral Europe. Available at: https://eur-lex.europa.eu/legal-content/EN/TXT/PDF/?uri=CELEX:52020DC0301&from=EN.

Flayac, C., Trably, E., Bernet, N., 2018. Microbial anodic consortia fed with fermentable substrates in microbial electrolysis cells: Significance of microbial structures. Bioelectrochemistry 123, 219–226. https://doi.org/10.1016/j.bioelechem.2018.05.009

Jia, X., Li, M., Wang, Y., Wu, Y., Zhu, L., Wang, X., Zhao, Y., 2020. Enhancement of hydrogen production and energy recovery through electro-fermentation from the dark fermentation effluent of food waste. Environ. Sci. Ecotechnology 1, 100006. https://doi.org/10.1016/j.ese.2019.100006

Kadier, A., Kalil, M.S., Chandrasekhar, K., Mohanakrishna, G., Saratale, G.D., Saratale, R.G., Kumar, G., Pugazhendhi, A., Sivagurunathan, P., 2018. Surpassing the current limitations of high purity H_2 production in microbial electrolysis cell (MECs): Strategies for inhibiting growth of methanogens. Bioelectrochemistry 119, 211–219. https://doi.org/10.1016/j.bioelechem.2017.09.014

Khongkliang, P., Jehlee, A., Kongjan, P., Reungsang, A., O-Thong, S., 2019. High efficient biohydrogen production from palm oil mill effluent by two-stage dark fermentation and microbial electrolysis under thermophilic condition. Int. J. Hydrogen Energy 44, 31841–31852. https://doi.org/10.1016/j.ijhydene.2019.10.022

Khongkliang, P., Kongjan, P., Utarapichat, B., Reungsang, A., O-Thong, S., 2017. Continuous hydrogen production from cassava starch processing wastewater by two-stage thermophilic dark fermentation and microbial electrolysis. Int. J. Hydrogen Energy 42, 27584–27592. https://doi.org/10.1016/j.ijhydene.2017.06.145

Koul, Y., Devda, V., Varjani, S., Guo, W., Hao Ngo, H., Taherzadeh, M.J., Chang, J.-S., C Wong, J.W., Bilal, M., Kim, S.-H., Bui, X.-T., Parra-Saldívar, R., Chi Minh, H., Chi Minh City, H., 2022. Microbial electrolysis: a promising approach for treatment and resource recovery from industrial wastewater. Bioengineered 13. https://doi.org/10.1080/21655979.2022.2051842

Lalaurette, E., Thammannagowda, S., Mohagheghi, A., Maness, P.C., Logan, B.E., 2009. Hydrogen production from cellulose in a two-stage process combining fermentation and electrohydrogenesis. Int. J. Hydrogen Energy 34, 6201–6210. https://doi.org/10.1016/j.ijhydene.2009.05.112

Lee, C., Lee, S., Han, S.K., Hwang, S., 2014. Effect of operational pH on biohydrogen production from food waste using anaerobic batch reactors. WATER Sci. Technol. 69, 1886–1893. https://doi.org/10.2166/wst.2014.097

Marone, A., Ayala-Campos, O.R., Trably, E., Carmona-Martínez, A.A., Moscoviz, R., Latrille, E., Steyer, J.P., Alcaraz-Gonzalez, V., Bernet, N., 2017. Coupling dark fermentation and microbial electrolysis to enhance bio-hydrogen production from agro-industrial wastewaters and by-products in a bio-refinery framework. Int. J. Hydrogen Energy 42, 1609–1621. https://doi.org/10.1016/j.ijhydene.2016.09.166

Murali, N., Srinivas, K., Ahring, B.K., 2021. Increasing the production of volatile fatty acids from corn stover using bioaugmentation of a mixed rumen culture with homoacetogenic bacteria. Microorganisms 9, 1–13. https://doi.org/10.3390/microorganisms9020337

Noguer, M.C., Magdalena, J.A., Bernet, N., Escudié, R., Trably, E., 2022. Enhanced Fermentative Hydrogen Production from Food Waste in Continuous Reactor after Butyric Acid Treatment. Energies. https://doi.org/10.3390/en15114048

Parthiba Karthikeyan, O., Trably, E., Mehariya, S., Bernet, N., Wong, J.W.C., Carrere, H., 2018. Pretreatment of food waste for methane and hydrogen recovery: A review. Bioresour. Technol. 249, 1025–1039. https://doi.org/10.1016/j.biortech.2017.09.105

Paul, D., Noori, M.T., Rajesh, P.P., Ghangrekar, M.M., Mitra, A., 2018. Modification of carbon felt anode with graphene oxide-zeolite composite for enhancing the performance of microbial fuel cell. Sustain. Energy Technol. Assessments 26, 77–82. https://doi.org/10.1016/j.seta.2017.10.001

Tang, T., Chen, Y., Liu, M., Du, Y., Tan, Y., 2022. Effect of pH on the performance of hydrogen production by dark fermentation coupled denitrification. Environ. Res. 208. https://doi.org/10.1016/j.envres.2021.112663

Tapia-Venegas, E., Ramirez-Morales, J.E., Silva-Illanes, F., Toledo-Alarcón, J., Paillet, F., Escudie, R., Lay, C.H., Chu, C.Y., Leu, H.J., Marone, A., Lin, C.Y., Kim, D.H., Trably, E., Ruiz-Filippi, G., 2015. Biohydrogen production by dark fermentation: scaling-up and technologies integration for a sustainable system. Rev. Environ. Sci. Biotechnol. 14, 761–785. https://doi.org/10.1007/s11157-015-9383-5

The European Comission, 2011. Commission Regulation (EU) No 142/2011 of 25 February 2011 implementing Regulation (EC) No 1069/2009 of the European Parliament and of the Council laying down health rules as regards animal by-products and derived products not intended for human consumpti. Off. J. Eur. Union L 54, 1–254.

Tian, H., Li, J., Yan, M., Tong, Y.W., Wang, C.H., Wang, X., 2019. Organic waste to biohydrogen: A critical review from technological development and environmental impact analysis perspective. Appl. Energy 256, 113961. https://doi.org/10.1016/j.apenergy.2019.113961

Yang, N., Hafez, H., Nakhla, G., 2015. Impact of volatile fatty acids on microbial electrolysis cell performance. Bioresour. Technol. 193, 449–455. https://doi.org/https://doi.org/10.1016/j.biortech.2015.06.124

Zagklis, D., Papadionysiou, M., Tsigkou, K., Tsafrakidou, P., Zafiri, C., Kornaros, M., 2021. Effect of pH on the economic potential of dark fermentation products from used disposable nappies and expired food products. Appl. Sci. 11. https://doi.org/10.3390/app11094099

Zhen, G., Lu, X., Kumar, G., Bakonyi, P., Xu, K., Zhao, Y., 2017. Microbial electrolysis cell platform for simultaneous waste biorefinery and clean electrofuels generation: Current

situation, challenges and future perspectives. Prog. Energy Combust. Sci. 63, 119–145. https://doi.org/10.1016/J.PECS.2017.07.003

FIGURE CAPTIONS

Figure 1. A: Total hydrogen production (mL H_2/g VS) obtained at the different pH values assessed; B: Organic matter conversion into organic acids (%) and concentration (g COD/L) in the fermentations assessed at pH values from 5 to 8.

Figure 2. Organic matter conversion into organic acids (%) and concentration (g COD/L) in the fermentations assessed at different temperatures (25, 37, and 50 °C).

Figure 3. Organic acids evolution along the experimental time for the effluents coming from DF at pH 7 (A-B) and at pH 5.5 (C-D)

Figure 4. Energy output generated considering the DF and MEC coupling at the two pH values assessed being A and B the two batches from DF at pH 7 and C and D those coming from DF at pH 5.5.

Table 1. Hydrogen production in MECs using as carbon source the different VFA distribution obtained after DF at two different pH values (7 and 5.5)

	pH 7 - A	**pH 7 - B**	**pH 5.5 - A**	**pH 5.5 - B**
CODin (g)	2.49	1.53	3.24	4.04
Initial C2/C4 ratio	1.949	1.808	0.603	0.537
H_2 Total (L)	1.83	0.87	0.56	0.75
Production rate (L H_2/d·L)*	0.083	0.041	0.031	0.026
VFAs removal (%)	84.5	95.0	28.7	59.0
COD-H_2/CODin (%)	52.72	40.72	12.44	13.38
mL H_2/ g CODin	733.14	566.28	172.98	186.07
mL H_2/ g VFAaa-eq*	1060.49	817.14	410.33	550.00
CE (%)	83.35	91.42	11.99	7.89
r_{cat} (%)	65.39	56.91	56.18	37.63
r_{H2}	54.50	52.03	6.76	2.97

*Production rate (L H_2/d*L) taking into account the first 21 days of experiment; *g VFAaa-eq; g VFA in acetic acid equivalents

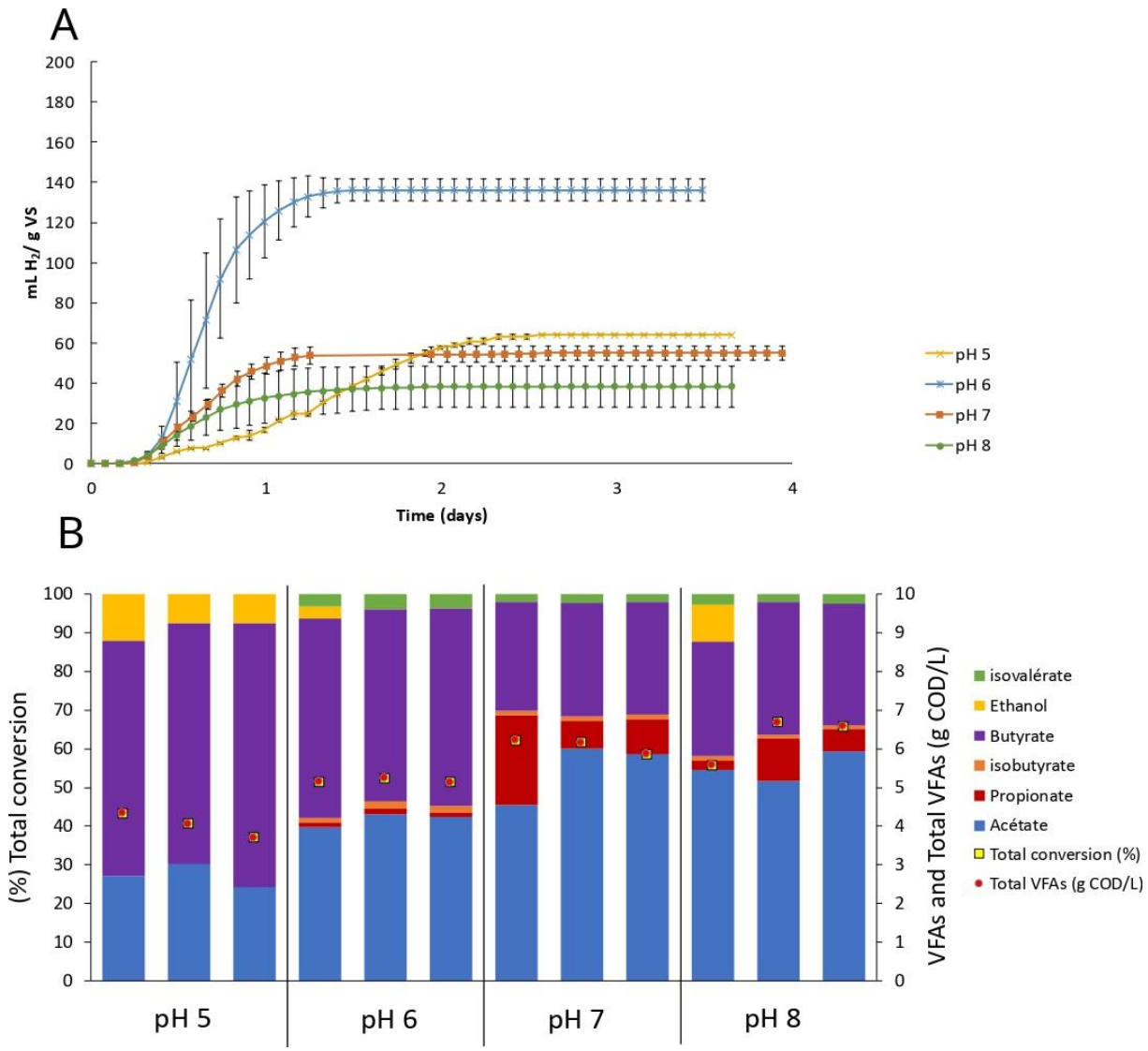

Figure 1. A: Total hydrogen production (mL H_2/g VS) obtained at the different pH values assessed; B: Organic matter conversion into organic acids (%) and concentration (g COD/L) in the fermentations assessed at pH values from 5 to 8.

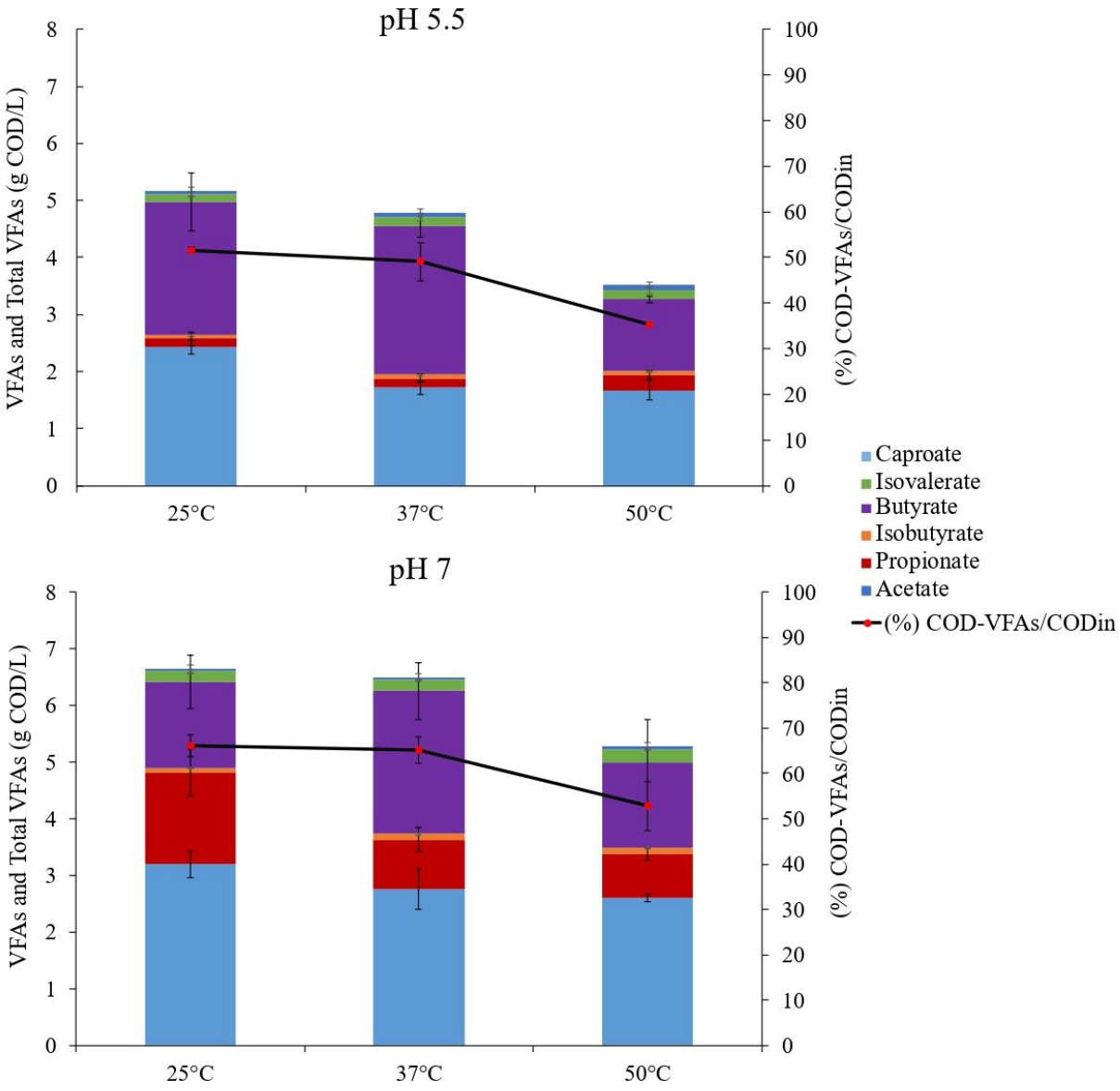

Figure 2. Organic matter conversion into organic acids (%) and concentration (g COD/L) in the fermentations assessed at different temperatures (25, 37, and 50 °C).

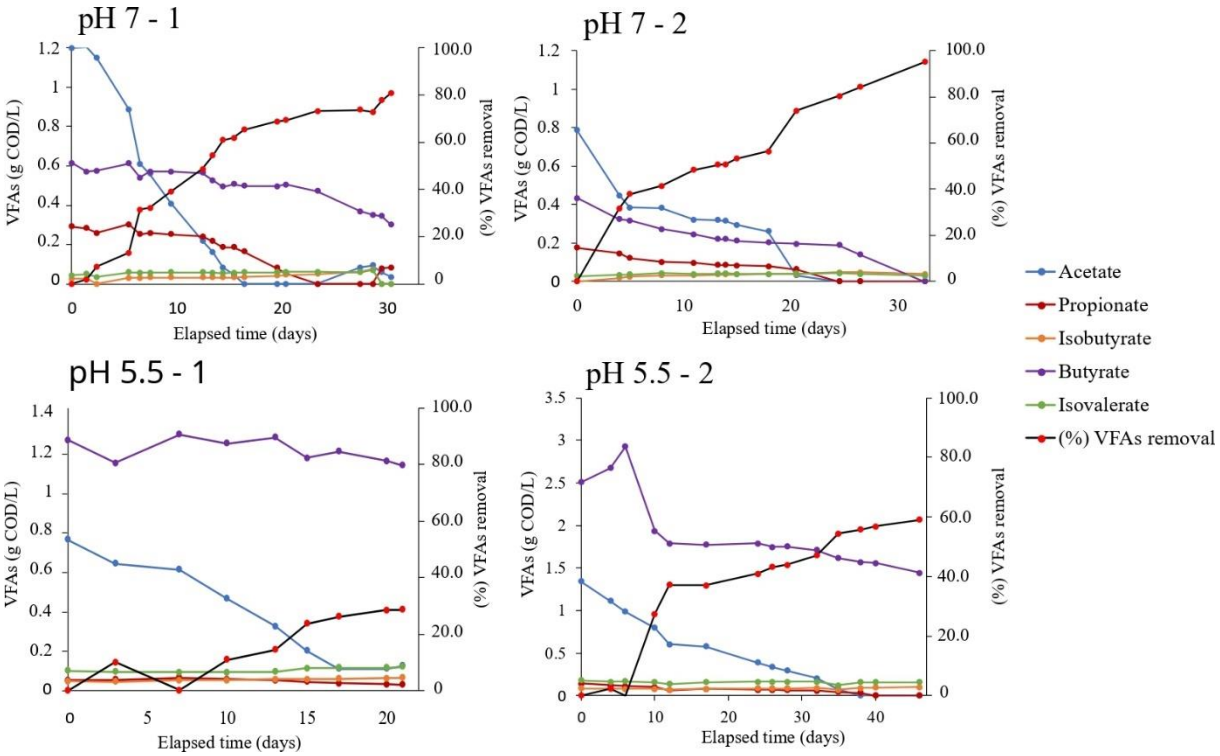

Figure 3. Organic acids evolution along the experimental time for the effluents coming from DF at pH 7 (A-B) and at pH 5.5 (C-D)

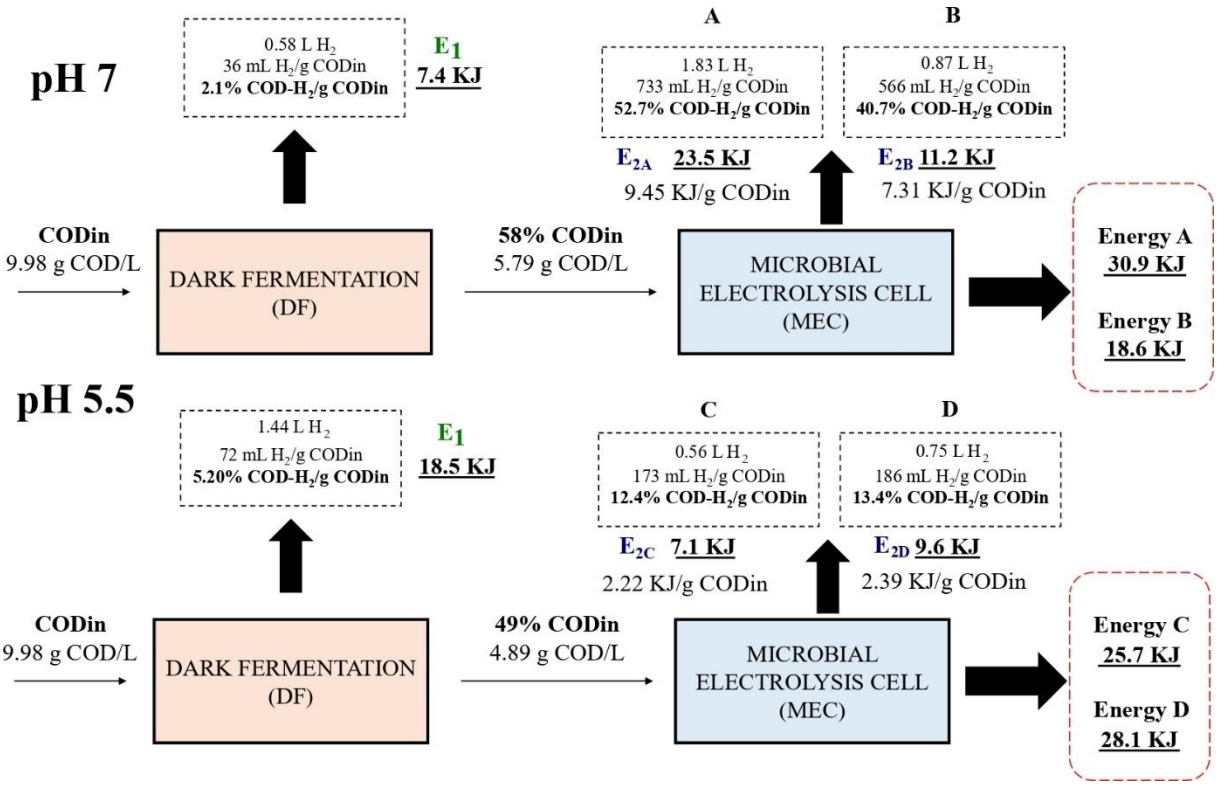

Figure 4. Energy output generated considering the DF and MEC coupling at the two pH values assessed being A and B the two batches from DF at pH 7 and C and D those coming from DF at pH 5.5.